

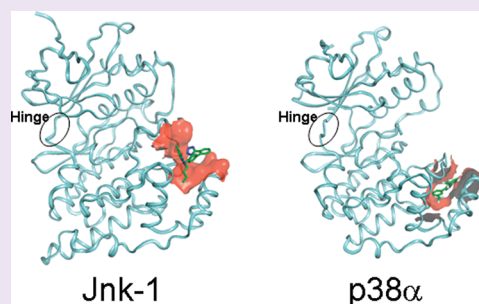
Discovery and Characterization of Non-ATP Site Inhibitors of the Mitogen Activated Protein (MAP) Kinases

Kenneth M. Comess,* Chaohong Sun, Cele Abad-Zapatero, Eric R. Goedken, Rebecca J. Gum, David W. Borhani, Maria Argiriadi, Duncan R. Groebe, Yong Jia, Jill E. Clampit, Deanna L. Haasch, Harriet T. Smith, Sanyi Wang, Danying Song, Michael L. Coen, Timothy E. Cloutier, Hua Tang, Xueheng Cheng, Christopher Quinn, Bo Liu, Zhili Xin, Gang Liu, Elizabeth H. Fry, Vincent Stoll, Teresa I. Ng, David Banach, Doug Marcotte, David J. Burns, David J. Calderwood, and Philip J. Hajduk

Global Pharmaceutical Research and Development, Abbott Laboratories, Abbott Park, Illinois 60064, United States

S Supporting Information

ABSTRACT: Inhibition of protein kinases has validated therapeutic utility for cancer, with at least seven kinase inhibitor drugs on the market. Protein kinase inhibition also has significant potential for a variety of other diseases, including diabetes, pain, cognition, and chronic inflammatory and immunologic diseases. However, as the vast majority of current approaches to kinase inhibition target the highly conserved ATP-binding site, the use of kinase inhibitors in treating nononcology diseases may require great selectivity for the target kinase. As protein kinases are signal transducers that are involved in binding to a variety of other proteins, targeting alternative, less conserved sites on the protein may provide an avenue for greater selectivity. Here we report an affinity-based, high-throughput screening technique that allows nonbiased interrogation of small molecule libraries for binding to all exposed sites on a protein surface. This approach was used to screen both the c-Jun N-terminal protein kinase Jnk-1 (involved in insulin signaling) and p38 α (involved in the formation of TNF α and other cytokines). In addition to canonical ATP-site ligands, compounds were identified that bind to novel allosteric sites. The nature, biological relevance, and mode of binding of these ligands were extensively characterized using two-dimensional $^1\text{H}/^{13}\text{C}$ NMR spectroscopy, protein X-ray crystallography, surface plasmon resonance, and direct enzymatic activity and activation cascade assays. Jnk-1 and p38 α both belong to the MAP kinase family, and the allosteric ligands for both targets bind similarly on a ledge of the protein surface exposed by the MAP insertion present in the CMGC family of protein kinases and distant from the active site. Medicinal chemistry studies resulted in an improved Jnk-1 ligand able to increase adiponectin secretion in human adipocytes and increase insulin-induced protein kinase PKB phosphorylation in human hepatocytes, in similar fashion to Jnk-1 siRNA and to rosiglitazone treatment. Together, the data suggest that these new ligand series bind to a novel, allosteric, and physiologically relevant site and therefore represent a unique approach to identify kinase inhibitors.



With the successful launch of Gleevec, Iressa, Tarceva, and other kinase inhibitors, protein kinases have rapidly become one of the most important groups of drug targets.¹ In fact, there are now more than 200 kinase inhibitors in clinical development (Prous Science Integrity, <http://www.prous.com/integrity/>), and the preclinical target portfolio of nearly every major pharmaceutical company contains a substantial fraction of protein kinases. Because of their nearly ubiquitous involvement in cellular signaling, kinases potentially play a role in a large number of disease states. Furthermore, the identification of reversible inhibitors of kinases presents an especially attractive paradigm for a medicinal chemist as compared with other types of common molecular targets such as proteases, voltage-gated ion channels, and transporters because of the ease of assay development and interpretation and inherent druggability.² For protein kinases, the vast majority of reported inhibitors bind to the highly conserved ATP binding site.³ This site has proven highly capable of binding drug-like molecules and is also functionally relevant.

In fact, the typical high-throughput screening approach to identification of new small molecule kinase inhibitors involves targeting of the ATP binding site because of the ease of assay design and likelihood of finding hits.^{4,5}

Unfortunately, however, targeting the ATP site of protein kinases for drug development has several limitations. First, the ease of hit identification and similarity of the ATP binding site across many kinase targets often leads to problems with specificity, where one compound may potentially inhibit multiple kinases. Although targeted polypharmacology (referring to the intentional targeting of multiple proteins) has shown promise in human clinical intervention, particularly in cancer therapy,^{6,7} it is difficult to predict or tune the pattern of inhibition across the more than 500 kinases comprising the kinome.⁸ In fact, favorable selectivity patterns are frequently serendipitous. While

Received: August 27, 2010

Accepted: November 23, 2010

Published: November 23, 2010

such serendipity can lead to new applications,⁹ more often the result is unexpected toxicity or side effects mediated through these off-target interactions.¹⁰ A second consequence of the conserved nature of the ATP binding site is the highly congested intellectual property (IP) landscape for kinase inhibitors, making it difficult to discover an entity chemically distinct from existing prior art. A recent analysis indicated that more than 10,000 patents and patent applications covering protein kinase inhibitors have been published since 2001,¹¹ highlighting the challenge for the drug researcher hoping to find novel chemical matter. Finally, in certain cases, it may be very difficult to identify inhibitors with sufficient potency to effectively compete with endogenous ATP, which is typically present at a concentration of 1 mM in the cell. This is especially true when the K_m value for ATP is very low ($\leq 1 \mu\text{M}$); inhibitors with picomolar potency may be required to be efficacious.

Given these limitations, there is a general need for alternative approaches to kinase inhibition in order to better control selectivity, provide clear IP protection, and circumvent the need to compete with endogenous ATP. In this article we describe the affinity-based discovery of inhibitors that bind at sites distinct from the active site in two mitogen activated protein kinases (MAPKs): the c-Jun N-terminal kinase 1 (Jnk-1) and p38 α . Detailed NMR and high resolution crystallographic analyses revealed that the inhibitors bind to sites associated with the MAP insertion within the structure of Jnk-1 and p38 α . The Jnk-1 compound is active and noncompetitive with ATP in activation cascade assays, suggesting that it is able to block activation of Jnk-1 by its respective upstream MEK kinases. Thus, such compounds may represent novel approaches for targeting the inactive form of MAP kinases with the potential for improved selectivity, cellular potency, and safety.

RESULTS AND DISCUSSION

Application to Jnk-1. Jnk-1 is a serine/threonine protein kinase that has been implicated in the pathology of type 2 diabetes, viral infection, and neuroprotection against stroke.¹² One of the substrates of Jnk-1 is Insulin-Receptor-Substrate-1 (IRS-1), which upon phosphorylation at Ser307 results in a down-regulation of insulin signaling *in vitro*.^{13,14} In addition, Jnk-1 knockout mice maintain lower fasting plasma glucose and insulin levels than their wild-type littermates when subject to a high fat diet, suggesting that the null animals are protected from developing obesity-induced insulin resistance.¹⁵ On the basis of these data, multiple companies have pursued inhibitors of Jnk-1 for the treatment of type 2 diabetes.^{12,16–27} All but one of the currently described inhibitor strategies are directed toward the ATP site, with various degrees of specificity. The non-ATP site inhibitors are peptides or small molecules based on interference with Jnk-1-JIP (Jnk-Interacting Protein) protein–protein interactions.^{18,27}

Affinity Screening and Characterization. The ATP site inhibitor series developed at Abbott (exemplified by compound 1, see Figure 1) was initially discovered through a conventional activity screen.²³ The research team also was interested in alternate mechanisms that might act on Jnk-1 at the site of interaction with the upstream JIP scaffolding protein or upstream MKK7 or MKK4 activating kinases, and in order to augment this screen and potentially identify novel inhibitors, an affinity-based screen was performed against the unphosphorylated (and therefore inactive) Jnk-1 protein using affinity selection followed by

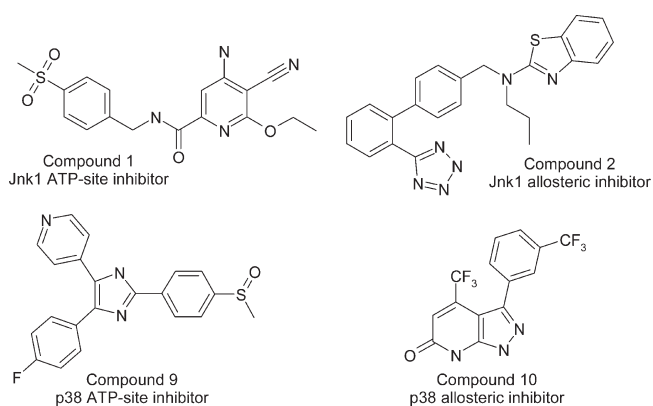


Figure 1. Structures of ATP-site (compounds 1 and 9) and allosteric site (compounds 2 and 10) inhibitors of Jnk-1 (compounds 1 and 2) and p38 α (compounds 9 and 10) as described in the text.

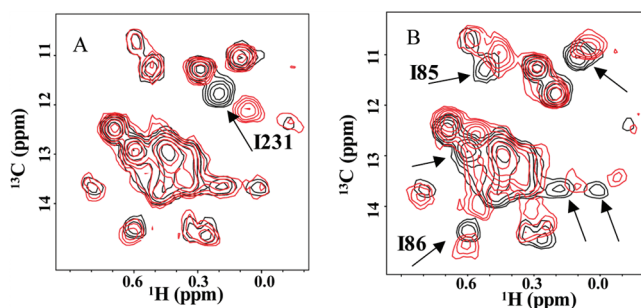
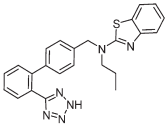
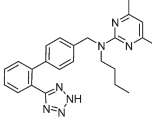


Figure 2. Selected region of ¹H/¹³C-HSQC spectra acquired on 50 μM ¹³CH₃-IVL-labeled Jnk-1 in the absence (black contours) and presence (red contours) of (A) 100 μM compound 2 and (B) 100 μM SP600125 (PDB entry 1uki). The assignments for selected cross-peaks are indicated as identified by the X-ray structure of the Jnk-1:compound 3 complex. The fingerprint of NMR spectral shifts in the HSQC spectrum is different for compound 2, a typical biaryl tetrazole, than that of SP600125 (a known ATP-binding site inhibitor).

mass spectroscopy (ASMS^{28,29}). Briefly, diverse large mixtures of compounds were added to inactive Jnk-1 protein in solution, equilibration was allowed at RT, and very weak ligands and nonbinders were separated from ligands by several rounds of ultrafiltration through a 10,000 Da molecular weight cutoff membrane, followed by restoration of the original volume. At equilibrium, the protein concentration determines the screening stringency; for example, a 1 μM K_D ligand is 50% bound at 1 μM protein concentration yet would be 90% bound at 10 μM protein concentration. Since the volume is reduced during ultrafiltration steps, the protein concentration concomitantly increases and results in enrichment of the bound species without significant loss due to kinetic (dissociation rate) effects. Mass spectrometry then was used to directly identify the ligands after a terminal chemical extraction step.²⁸

A library of ~500,000 small molecules was screened, from which 68 candidate ligands were identified. To confirm binding and provide information on the binding site location, high-resolution NMR binding studies were conducted using ¹³C-methyl-labeled inactive JNK1 α 1 (residues 1–364, Thr183-Glu, Tyr185Glu). From the set of 68 candidate ligands, 41 were confirmed as ligands for the protein. Interestingly, as illustrated in Figure 2, two very distinct chemical shift patterns were observed for different classes of ligands. ATP site ligands, for

Table 1. Biaryl-tetrazole Affinity and Coupled Assay Data for JNK Isoforms and Related MAP Kinase Proteins

No.	Structure	IC ₅₀ ^a Jnk-1	IC ₅₀ ^a MKK7cp ^b	K _d ^c Jnk1-u ^d	K _d ^c Jnk1-a ^e	K _d ^c p38α-u ^d	K _d ^c ERK2-u ^d
2		> 100	7.8	11	>50	18	18
3		62	7.7	16	>50	17	32

^a IC₅₀ values (in μM) from activity assays. ^b Coupled MKK7-Jnk-1 activity assay. ^c K_d values (in μM) from ASMS. ^d Unactivated protein. ^e Activated protein.

example SP600125,¹⁶ exhibit a characteristic pattern of shifts typically perturbing the resonances of Ile85 and Ile86, among others (Figure 2B). The majority of confirmed ligands from the ASMS screen (34 of 41 tested) exhibit this type of shift pattern and therefore bind to the ATP binding site. Two compounds (compounds 2 and 3, Table 1), however, perturb the methyl resonance of Ile231, but not Ile85 and Ile86, suggesting that they bind exclusively to a different site on the protein (Figure 2). The remaining five compounds appeared to occupy both the ATP and non-ATP site to varying degrees. NMR binding competition studies between compound 1 (an ATP site binder) and compound 2 (a non-ATP site binder) indicate that these compounds can bind simultaneously to the protein, and they do not compete with each other (data not shown). This suggests that binding to the novel site does not prevent binding to the ATP site through allosteric modulation.

As shown in Table 1, compounds 2 and 3 (which bind exclusively to the non-ATP site) did not exhibit any activity in a conventional biochemical assay for Jnk-1 (IC₅₀ values >50 μM). This was confirmed in affinity binding studies using phosphorylated (e.g., active) Jnk-1, where no compound binding could be detected (Table 1). Thus, these compounds appear to bind exclusively to the inactive form of the protein. Binding of typical ATP-site inhibitors appeared to be unaffected by the phosphorylation state, as evidenced by SP600125 binding with high affinity to the inactive, unphosphorylated protein (Figure 2). As all members of the MAPK family are activated by upstream dual-specificity kinases, a cascade assay was developed in which inactive Jnk-1 was activated by its upstream partner MKK7. Compounds 2 and 3 were in fact active in this assay, exhibiting IC₅₀ values comparable to their affinities for Jnk-1 (Table 1). Direct inhibition studies on MKK7 indicate no evidence of activity on the upstream kinase (data not shown). Together, the Jnk-1 ASMS, NMR, activity assay, and cascade assay data support the premise that the biaryl tetrazole compounds bind to a novel site on Jnk-1 that inhibits the activation of Jnk-1 by MKK7.

Structural Characterization. Several X-ray crystal structures of Jnk-1¹⁷ and Jnk-3³⁰ have been determined when associated with the JIP1 common docking site undecapeptide and in complex with several classes of JNK inhibitors.³¹ Our laboratory has also reported the structures of potent and selective ATP-competitive inhibitors of Jnk-1 bound to the α1 isoform, focusing on the medicinal chemistry aspects of inhibitor design.^{22–25} In order to characterize the novel binding site in more detail,

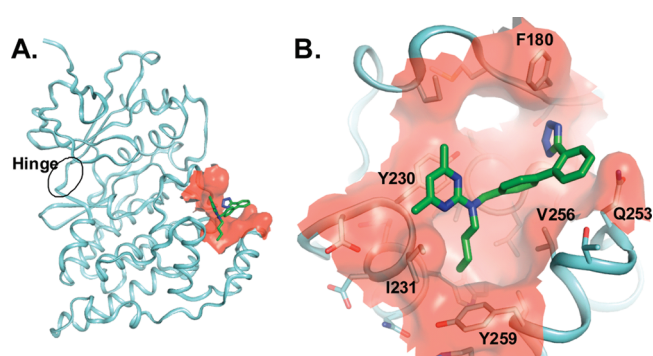


Figure 3. X-ray crystal structure of Jnk-1 (cyan ribbons) complexed to compound 3 (colored by atom type). As shown in panel A, the compound binding site (shaded in red) is distant from the ATP-binding site (hinge region; denoted by the circle) and is located in the MAP insert region. The close-up view in panel B highlights the amino acids involved in the interaction.

crystallographic studies of Jnk-1 in the presence and absence of compound 3 were performed. As shown in Figure 3A, the compound binds on a ledge provided by the MAP insertion on the surface of the protein. The “northern” boundary of the binding pocket (see Figure 3B) is provided by residues in the activation loop, particularly Ser179 to Glu185, that exhibit a different conformation than the one found in the apo enzyme. This supports the biochemical data, which indicate that phosphorylation of this loop can abrogate compound binding, presumably due to a conformational change. The “southern” limit of the pocket is provided by residues from the MAP insertion (residues Gly242 to Ala267), especially Val256 and Tyr259. The “western” side of the pocket provides distinct interactions with amino acids that vary the most among the different isoforms (Met218–Trp234). Of note among these residues are Ile231 and especially Tyr230 (His in Jnk-1β, Jnk-2α isoforms), whose side chain conformation is different from the apoenzyme form and provides a ring stacking interaction with the dimethyl pyrimidine ring of 3. This conformational change results in a tight “hydrophobic bend” that accommodates the dimethyl pyrimidine portion of the ligand between Ile231 and Tyr230. The close van der Waals interaction of the compound with Ile231 explains the sensitivity of the NMR spectra to this class of compounds. The butyl moiety of 3 is inserted into the broad hydrophobic pocket containing Trp234 at its floor. The “eastern” side of the pocket is less

Table 2. Selected SAR of the Biaryl-tetrazole Based Jnk-1 Activation Inhibitors

No.	Structure	IC ₅₀ (MKK7-Jnk1) ^a	IC ₅₀ (Jnk1) ^b	EC ₅₀ (P-cJun) ^c
2		7.8	>100	>30
3		7.7	>10	>30
4		2.9	>100	>10
5		2.8	68.6	>10
6		3.1	ND	>10
7		3.8	>100	4.0
8		4.7	82.3	>10

^a IC₅₀ values (in μM) in the coupled MKK7-Jnk-1 activity assay. ^b IC₅₀ values (in μM) in a direct Jnk-1 activity assay. ^c EC₅₀ values (in μM) for inhibiting TNF α -stimulated cJun phosphorylation in HepG2 cells

restricted and accommodates the biaryl tetrazole moiety in two different conformations. The nearest residues (Gln253 and Thr255) originate from the N-terminus of the second helix of the MAP insertion (α_{2L14}) but do not seem to make any specific interactions with the tetrazole group of compound 3.

Design of Cell-Active Compounds. Neither compound 2 nor 3 exhibited cellular inhibition of cytokine (TNF α) stimulated Jnk-1 activity in HepG2 cells. Likely causes for this are the large size and lipophilicity of the ligands. However, as shown by the crystal structure, much of compound 3 is solvent-exposed, suggesting several strategies for medicinal chemistry optimization. The two major sources of binding affinity appear to be a stacking interaction between the pyrimidine ring and Tyr230 of Jnk-1 and partial occupancy of the hydrophobic channel by the compound's *n*-butyl side chain. The aryl-tetrazole moiety seems to be mobile and does not contribute much to the interaction with Jnk-1. Several compounds therefore were synthesized to reduce the size of the compounds while maintaining critical interactions. As shown in Table 2, the entire terminal aryl-tetrazole group could be replaced with a phenol group (6) or pyridine group (8) without losing the ability to inhibit JNK1 α 1

activation. Further efforts resulted in compound 7, in which only one terminal aryl group is needed for inhibiting JNK1 α 1 activation by MKK7. This smaller, less lipophilic compound in fact exhibits robust cellular activity. As shown in Figure 4, both the conventional ATP site inhibitor (1) and compound 7 inhibited phosphorylation of the downstream target of Jnk-1 (c-Jun), but only compound 7 inhibited phosphorylation (activation) of Jnk-1 itself (Figure 4A). Thus, the new inhibitors bind to a new site on Jnk-1 and exhibit cellular activity through a mechanism distinct from inhibition of catalytic activity of Jnk-1 itself.

Application to p38 α . Like the Jnk enzymes, p38 is a serine/threonine protein kinase in the mitogen-activated protein kinase (MAPK) family. Jnk-1 is also known as MAPK8, and p38 α is MAPK14.³² There are four isoforms of p38 (p38 α , p38 β , p38 γ , and p38 δ), and p38 α is considered the key isoform involved in modulating inflammatory response in rheumatoid arthritis^{32,33} and inflammatory pain.³⁴ As with Jnk-1, there are a number of small molecule antagonists described in the literature (as exemplified by compound 9) (SB 203580)³⁵ but only one compound series that does not bind exclusively at the ATP site, represented by the clinical candidate BIRB-796.³⁶ This compound binds adjacent to the active site and directly inhibits enzymatic activity by affecting the conformation of the ATP site.³⁷ Additional, more distant sites for allosteric binding on p38 α kinase have been predicted using an additive free energy computational model,³⁸ and we were interested in pursuing an unbiased affinity-based high-throughput screening strategy to access these or other sites for additional lead generation opportunities. By augmenting traditional lead discovery strategies, small molecule leads with novel chemical structures and activity patterns might be obtained.

Affinity Screening and Characterization. The p38 α enzyme used for ASMS was partially phosphorylated (activated) prior to the high-throughput screen. While the inactive protein screening strategy for Jnk-1 was selected to be complementary to a concurrent activity-based HTS campaign, a companion activity-based screen was not run for p38 α . We wished therefore to survey the screening library in an unrestricted manner in order to have the best opportunity to discover ligands for both activated and unactivated p38 α protein. The screening sample contained an approximately 40/40/20 mixture of non-, mono-, and diphosphorylated species and was validated for use in the ASMS screen by testing compounds SB220025,³⁹ VX745,⁴⁰ and BIRB-796.⁴⁰ All three compounds demonstrated reproducible tight binding and estimated K_D values below the input target concentration of 6 μM .²⁸ Approximately 520,000 unique compounds were evaluated in mixtures using a protein concentration of 6 μM , and 145 compounds were found to bind with measurable affinity. Many familiar ATP competitive p38 α chemotypes were found in the hit set, including diaryl ureas, aryl-heteroaryl ureas, pyrazoles, imidazoles, quinazolines, piperidine amides, benzophenones, aryl pyrazoles, and halophenols.³² Additional novel chemotypes also were identified and subsequently characterized as described below.

¹³C-Methyl-labeled, unphosphorylated p38 α was used to characterize a set of 68 ASMS hits using two-dimensional ¹³C-¹H NMR. Out of the 68 compounds tested, 39 compounds were confirmed as ligands for p38 α . Similar to Jnk-1, two distinct chemical shift patterns were observed for different classes of compounds (see Figure 5). The majority of confirmed ligands showed a chemical shift pattern similar to that observed with an ATP site-binding ligand and therefore likely bind to the ATP site.

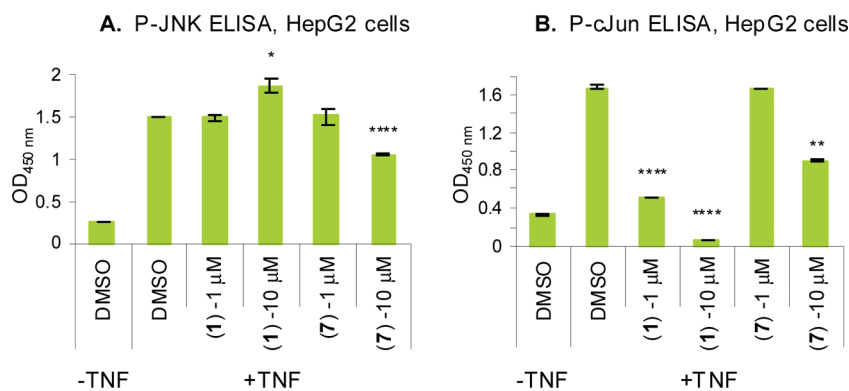


Figure 4. Quantitation of phosphorylated (A) Jnk-1 and (B) cJun in human hepatocyte cells (HepG2) after activation by TNF α and inhibition by compound 1 (ATP-competitive) or compound 7 (non-ATP competitive) at 1 and 10 μ M. * $p < 0.05$, ** $p < 0.01$, *** $p < 0.001$, **** $p < 0.0001$. Assay details as described in Methods.

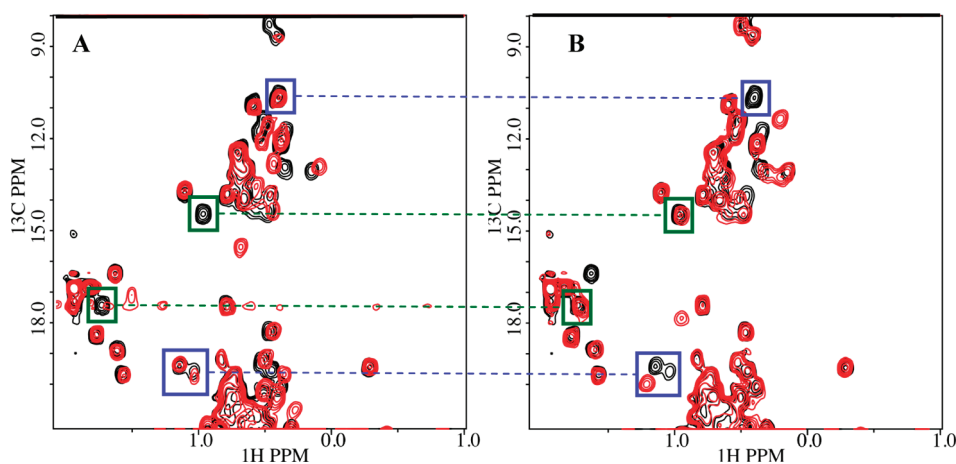


Figure 5. Selected region of $^1\text{H}/^{13}\text{C}$ -HSQC spectra acquired on 50 μ M $^{13}\text{C}_3$ -IVL-labeled p38 α in the absence (black contours) and presence (red contours) of (A) 100 μ M compound 9 and (B) 100 μ M compound 10. The fingerprint of NMR spectral shifts in the HSQC spectrum is different for compound 9 (a known ATP-site inhibitor, highlighted with green boxes) than compound 10 (highlighted with blue boxes).

Two compounds, however, including compound 10, shifted a different set of peaks, suggesting that they bind at a different site of the protein (Figure 5). NMR competition studies also showed that an ATP-site binder (compound 9) and compound 10 could bind simultaneously to the protein (data not shown). This result was supported by surface plasmon resonance experiments using a Biacore T100 instrument. Unphosphorylated p38 α was immobilized on a CMS chip through amine coupling. Compound 9 exhibited dose-dependent sensorgrams with an apparent K_D value of 14 nM, consistent with its reported K_i of 20 nM.⁴¹ Compound 10 also exhibited binding, and although its low solubility precluded acquisition of a full dose–response curve, extrapolation from the 10 μ M concentrations yielded a K_D value of 10 μ M. Competition experiments were performed by sequentially injecting compound 9 at 100 nM, compound 10 at 10 μ M, and a mixture of compound 9 (100 nM) and compound 10 (10 μ M). As shown in Figure 6, the observed signal from the mixture is the sum of individual responses from the two compounds, suggesting that these two compounds bind to the protein simultaneously.

Structural Characterization. The co-crystal structure of compound 10 with p38 α revealed that, as also seen in Jnk-1, the molecule is bound to a cleft formed by the MAP kinase insert on the C lobe of the kinase (see Figure 7). The site is located about 30 Å away from the canonical ATP site and is composed of two

α -helices connected by a short loop. Compared with the apo-protein structure, a local reorganization of both loop 12⁴² (containing Trp197 (Figure 7B)) and the loop connecting MAP insert helices α_{1L14} and α_{2L14} (residues from Ile250 to Glu254) opens up a groove in the protein allowing compound 10 to bind. The movement of loop 12 reorients Trp197 (Figure 7B), which then forms a face-to-face stacking interaction with the fused 6/5 pyrazolopyridone ring of compound 10. In addition, the pyridone carbonyl forms an H-bond with the backbone amide N–H of Ser252 located on a short loop between helices α_{1L14} and α_{2L14} . The 3-(3-(trifluoromethyl)) phenyl group appears twisted by the adjacent 4-trifluoromethyl group and points toward a cavernous hydrophobic pocket that extends to the base of helix G. This same groove formed by the MAP insert has been reported to bind various lipidic molecules such as arachidonic acid and 15-(S)-hydroxyeicosatetraenoic acids as well as *n*-octyl- β -glucopyranoside.⁴³ Interestingly, this pocket also bound a second copy of SB 203580 in the first reported crystal structure of p38 α ⁴⁴ in complex with SB 203580. However, characterization of SB 203580 here suggests that it only binds with high affinity to the ATP site (see above, Figure 5) and that binding to this distant site must be of low affinity, which is not detectable under our conditions.

Biochemical Characterization. Results of the biochemical characterization of compound 10 are shown in Table 3. Unlike

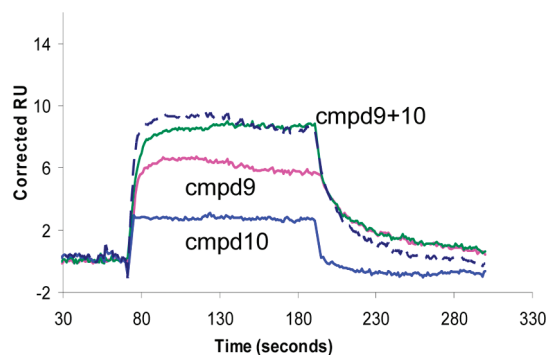


Figure 6. Biacore sensorgrams of 100 nM compound 9 (purple), 10 μ M compound 10 (blue), and 100 nM compound 9 + 10 μ M compound 10 (green) in the presence of immobilized p38 α protein.

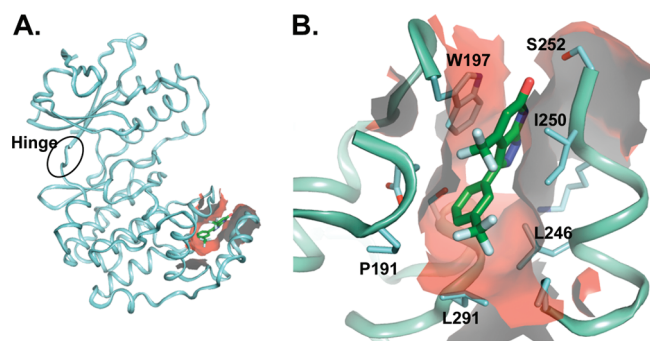


Figure 7. X-ray crystal structure of p38 α (cyan ribbons) complexed to compound 10 (colored by atom type). As shown in panel A, the compound binding site (shaded in red) is distant from the ATP-binding site (hinge region; denoted by the circle) and is located in the MAP insert region. The close-up view in panel B highlights the amino acids involved in the interaction.

the allosteric inhibitors of Jnk-1 described above, compound 10 directly inhibits p38 α with an IC_{50} value of 1.2 μ M in the presence of 0.1 μ M ATP.

Interestingly, the inhibition appears only slightly reduced (\sim 4-fold) when the ATP concentration is increased from 0.1 to 3 mM, which is smaller than the shift that is predicted by the Cheng–Prusoff equation (\sim 20-fold) and that is seen for ATP competitive inhibitors. However, poor compound solubility precludes accurate testing at concentrations of compound 10 needed to confirm such partial ATP competition. Compound 10 is active in the upstream (MKK6) and downstream (MK2) cascade assays with a potency similar to that against p38 α alone, suggesting no particular role of this compound in modulating the phosphorylation of p38 α or binding to MK2 as part of its inhibitory mechanism. The p38 α MAP kinase insert region is essentially isomorphous between uncomplexed p38 α and a heterodimeric complex of p38 α and MK2, consistent with the mechanism of inhibition being unrelated to the downstream protein–protein interaction.^{42,45,46}

The selectivity of compound 10 was also evaluated by screening against a panel of 129 protein kinases.⁴⁷ The compound exhibited no activity ($IC_{50} > 40 \mu$ M) against p38 β , p38 γ , and p38 δ (see Table 3), suggesting excellent selectivity even in these highly related isoforms. Among the other kinases in the panel (including 18 cytoplasmic tyrosine kinases, 23 receptor tyrosine kinases, and 88 serine/threonine kinases), the only targets that

Table 3. Biochemical Characterization of the Allosteric p38 α Inhibitor Compound 10

assay ([ATP])	IC_{50} (μ M)
p38 α (0.1 mM)	1.2
MKK6/p38 α cascade (0.1 mM)	0.8
p38 α /MK2 cascade (0.01 mM)	1.4
MKK6 (0.1 mM)	>100
MK2 (0.01 mM)	>40
p38 β (0.1 mM)	>40
p38 γ (0.1 mM)	>40
p38 δ (0.1 mM)	>40

showed activity at up to 10 μ M compound concentration were Pim1 ($K_i = 4.5 \mu$ M), Pim3 ($K_i = 1.9 \mu$ M), Map4k4 ($K_i = 4.7 \mu$ M), KHS ($K_i = 5.2 \mu$ M), Gsk3 β ($K_i = 4.9 \mu$ M), and BRSK1 ($K_i = 8.5 \mu$ M).

Comparison of Non-ATP Ligand Binding Sites in Jnk-1 and p38 α . We have described two lead discovery strategies employing high-throughput affinity-based screening to identify multiple classes of compounds capable of binding anywhere on the protein surface. Both the inactive and active kinase affinity-based ASMS approaches here build on previous studies done in our lab using ASMS.^{28,29,48–52} The Jnk-1 and p38 α screening campaigns were followed by orthogonal affinity (NMR and surface plasmon resonance) and biochemical characterization to identify the binding sites and finally by X-ray crystallographic analyses to understand the binding interactions at an atomic level. When applied to the two kinases Jnk-1 and p38 α , the majority of hits bound to the ATP-binding site. However, a small number of chemically interesting compounds exhibited binding to unique sites that could be quickly identified and further characterized. These novel binding sites offer new opportunities for further medicinal chemistry and the potential for intriguing insights into the biological roles of these enzymes.

In the case of Jnk-1, the inhibition mechanism via binding to the allosteric site appears reasonably clear. This site is accessible only in the inactive form of the protein, suggesting that phosphorylation of the activation loop leads to sufficiently large conformational changes to preclude compound binding. It therefore makes sense that binding to (and subsequent stabilization of) this site in unactivated Jnk-1 inhibits phosphorylation by MKK7. It is not clear from the available data whether this is direct inhibition of Jnk-1 binding to MKK7 or simply stabilization of an inactive form that resists phosphorylation. Either mechanism results in reduced levels of active Jnk-1 that manifests itself in cascade and cellular assays monitoring Jnk-1 activity.

The role for the allosteric site in p38 α is less clear. The direct inhibition of p38 α activity by compound 10 potentially suggests a mechanism distinct from that of the novel Jnk-1 compounds, perhaps through true allosteric modulation of either ATP or substrate binding. While the X-ray crystal structure did indicate some evidence of compound 10 binding to the ATP site (data not shown), the density was weak, and all available affinity data (see Figures 5 and 6) are consistent with the fact that the high-affinity binding site is the allosteric site, with affinities on the same order as the inhibitory activity. There is no suggestion from the crystal structure of p38 α with compound 10, when compared to that of Jnk-1 with compound 3, of why this compound may be working through a different mechanism. The physical basis and mechanism for inhibition from the distant binding site cannot be

defined with the available structural data, but it does present an intriguing opportunity for modulating activity without direct competition for binding to the highly conserved “hinge region” of the protein kinase.

The similarity in binding sites for the Jnk-1 and p38 α inhibitors is striking, as can be appreciated by comparing Figures 3A and 7A. Both compounds bind to a site that exists only due to the MAP insert region in these two kinases. This suggests that the compounds described here have the potential to be exquisitely selective, especially against kinases that lack the MAP insert region. The Jnk-1 allosteric inhibitors exemplified by compounds 2 and 3 do exhibit affinity for other inactive MAP kinases (p38 α and ERK2; see Table 1), but no activity for these compounds has been observed for other kinases despite the fact that they have been screened against dozens of protein kinases through internal HTS campaigns. The allosteric p38 α inhibitor 10 has been profiled against 129 protein kinases. This compound exhibits excellent selectivity within the p38 isoforms (see Table 3) and exhibits only weak activity against 6 other kinases on the panel. Thus, these compounds represent excellent starting points for medicinal chemistry efforts aimed at the development of potent and selective inhibitors for the Jnk-1 and p38 α kinases. These data also suggest a general strategy for targeting these sites in other MAP kinases.

In summary, we have identified novel allosteric binders of Jnk-1 and p38 α through an affinity-based lead discovery campaign. The Jnk-1 inhibitors were synthetically improved to exhibit cellular activity consistent with preventing the activation of Jnk-1 by its upstream kinase, MKK7. The p38 α compound directly inhibits p38 α activity. Both classes of compounds represent attractive starting points for the design of potent and selective inhibitors for these proteins that not only may serve as excellent chemical biology tools for the investigation of the biological roles of these proteins but also may have therapeutic potential.

METHODS

Enzyme Cloning and Expression. The Jnk-1 gene was cloned from rat brain cDNA for high-throughput ASMS screening. A clone that matched the human variant JNK alpha 1, variant 2 (Genbank Accession no. L26318; reference sequence NM_002750) was chosen from the rat variants sequenced. The amino acid sequence matches the human variant selected for further assay and structural work. The construct was His-tagged at the amino terminus and expressed in insect Sf9 cells.

For enzymatic assays and crystallographic studies, C-terminal His-tagged constructs of human Jnk-1 were used: [JNK1 α 1 (1–364)]-6His and [JNK1 α 1, Thr183Glu, Tyr185Glu (1–364)]-6His, respectively. These constructs were transformed into the *E. coli* strain BL21(DE3). NMR studies were carried out on the latter form, grown in ¹³C-enriched minimal medium.⁵³

The p38 α isoform for high-throughput screening was cloned by PCR from a mammalian cell extract and aligns most closely with Genbank Accession no. AY335728. As with Jnk-1, a His-tag was placed at the amino terminus. The construct is denoted as 6His-[MAPK14 (1–360)]. The p38 α enzyme used for ASMS was recombinantly expressed in *E. coli*, purified, then activated by treatment with upstream kinase MKK6 and reperfired. The p38 α protein construct for NMR studies was grown in supplemented minimal medium as for Jnk-1.

Enzyme Purification and Biophysical Characterization. Jnk-1 isoforms were purified following the protocol of Heo *et al.*,¹⁷ with 1 mM Na₃ present in all buffers, nickel ProBond (Invitrogen) used as the IMAC affinity resin, and a Sephacryl S-300 column employed as the sizing media. For crystallization experiments, the JIP1 peptide was added

in a 5 \times molar excess, after sizing and prior to the final concentration, to stabilize the protein. JIP1 peptide was not included in purifications for ASMS. The Jnk-1 protein was confirmed as unactivated by using an antiphospho Jnk-1 antibody in Western blots. In comparison, recombinant rat Jnk-1 activated *in vitro* by the JNK upstream kinases MKK4 and MKK7 is at least 1000-fold more reactive with the antibody (data not shown). The p38 α isoform for high-throughput screening was activated prior to use by exposure to the upstream kinase MKK6 and was then reperfired.

Jnk-1 Enzyme Activity Assay. Jnk-1 kinase reactions were performed in 50 μ L volume containing 10 ng/well enzyme (4.4 nM), 1 μ M BT-GST-ATF2 substrate, and γ -[³³P]-ATP (5 μ M, 400 μ Ci/ μ mol) in a buffer containing 20 mM MOPS, pH 7.2, 2 mM EGTA, 10 mM MgCl₂, 0.1% Triton X-100, 1 mM dithiothreitol, in a 96-well polypropylene plate. Reactions were carried out at 15–20 °C and stopped after 60 min by the addition of 50 mM EDTA (final). Aliquots (30 μ L) of the quenched reactions were transferred to a Streptavidin FlashPlate (PerkinElmer) containing 170 μ L of PBS. Plates were incubated at RT for 30 min, washed 4 times with PBS, and then counted in a PerkinElmer Micro-Beta plate counter.

MKK7/Jnk-1 Activation Cascade Assay. Activation of Jnk-1 was done in a reaction volume of 50 μ L containing 150 ng of MKK7 (40.5 nM), 50 ng of unactivated Jnk-1 (22 nM), and 86 μ M ATP, in a buffer containing 50 mM Tris HCl, pH 7.5, 0.01 mM EGTA, 10 mM MgCl₂, and 0.1% 2-mercaptoethanol in a 96-well polypropylene plate. The reaction was carried out at 30 °C for 60 min. A 10 μ L aliquot of the reaction was then added as the enzyme in the Jnk-1 activity assay described previously.

p38 α Pathway Enzyme Activity Assays. p38 α kinase reactions were performed in a buffer containing 20 mM MOPS, pH 7.2, 5 mM EGTA, 10 mM MgCl₂, 0.01% Triton X-100, 5 mM β -phosphoglycerol, 1 mM dithiothreitol, and 1 mM sodium orthovanadate. Compounds were titrated from 0 to 50 μ M in a constant 5% DMSO and added to a reaction containing 20 ng/well activated p38 α (12 nM final), a varying amount of ATP, and 0.5 μ M biotinylated maltose binding protein peptide. Reactions were allowed to proceed for 60 min at RT and then quenched with 10 μ L/well of 500 mM EDTA after 60 min. Detection reagents were added to final concentrations of 15 ng of Eu³⁺-labeled antiphospho-MBP and 0.34 μ g of SAXL (Phycolink Streptavidin-Allophycocyanin acceptor, cat. no. PJ25S, Prozyme) per well, and the plates were incubated in the dark at 4 °C overnight prior to being read on a RUBYstar HTRF reader (BMG Labtech).

p38 β , p38 γ , and p38 δ kinase reactions were performed similarly, except p38 γ used a buffer containing 50 mM Tris-HCl, pH 7.5, 1 mM EGTA, 10 mM MgCl₂, 0.01% Brij-35, 2 mM dithiothreitol, and 5 mM β -glycero-phosphate and biotinylated full-length maltose binding protein (Upstate/Millipore cat. no. 13-111) was used as substrate. MK2 kinase assays were run in the same buffer as p38 α using a biotinylated CDC28 peptide as substrate and Eu³⁺-labeled detection antibody (Phospho-Ser 14-3-3 Binding Motif 4E2 Monoclonal Antibody from Cell Signaling Technology; cat. no. 9606) and Allophycocyanin-Streptavidin (Perkin-Elmer; cat. no. CR130-100). MKK6 kinase assays were run in the same buffer as p38 α using substrate and detection reagents from a KinEASE STK kit (Cisbio, Inc.). MKK6/p38 α cascade assays used MKK6 to phosphorylate unactivated p38 α , the activity of which was determined by subsequent phosphorylation of biotinylated maltose binding protein peptide, using the same detection reagents as the p38 α direct assay. p38 α /MK2 cascade assays used activated p38 α to phosphorylate unactivated MK2, the activity of which was determined by subsequent phosphorylation of biotinylated CDC28 peptide, using the same detection reagents as the MK2 direct assay.

Cell Assays. HepG2 human hepatoma cells (ATCC) were cultured in low glucose MEM supplemented with 1X NEAA, 1X sodium pyruvate, and 10% FBS (all from Invitrogen). Cells were plated at 5 \times 10⁴

cells/well in 500 μL complete media on 24-well collagen-coated plates and incubated overnight. Serial compound dilutions were made in DMSO at 100X then 5 μL were added directly to the media on the cells to make the indicated final concentrations (final DMSO concentration in media 1%). After 1 h, cells were stimulated with vehicle control or 20 ng/mL TNF α for 30 min and harvested in 70 μL of lysis buffer (TBS (54 mM Tris-HCl, pH 7.6, 150 mM NaCl, Sigma), 1% TritonX-100, Sigma), 0.5% Nonidet P-40 (Sigma), 0.25% sodium deoxycholate (Sigma), 1 mM EDTA, 1 mM EGTA (Sigma), 0.5 mM sodium fluoride (Sigma), 1 mM pervanadate (Sigma), 1 μM microcystin (Calbiochem), 1 mM AEBSF (Roche), 1 tablet Mini EDTA-free inhibitor cocktail (Roche)/10 mL lysis buffer) and frozen at $-80\text{ }^\circ\text{C}$ prior to use. P-cJun and P-JNK ELISAs were performed as described by the manufacturer (Cell Signaling Technology) using 50 μL cell extract.

Affinity Selection/Mass Spectrometry (ASMS). Affinity-based high-throughput screening was carried out on a collection of approximately 503,000 small organic compounds, in two stages. In the first stage, 210 large diverse compound mixtures (average of 2,400 compounds each) were allowed to equilibrate with purified protein in solution, at a concentration of 1.5 μM each compound and 10 μM Jnk-1 or 6 μM p38 α . The buffer for both screens comprised 50 mM Tris-HCl, pH 8.5, 150 mM NaCl, 3 mM DTT, and approximately 6% v/v DMSO. The equilibration steps were conducted in 400 μL volumes in disposable centrifugal filter tubes (Microcon YM-10, Millipore). By using either commercial centrifuge instruments or custom pressure-limited filtration devices,²⁸ the entire set of protein/compound mixtures in 210 tubes was then subjected in parallel to 10-fold concentration in approximately 30 min. Restoration of the volumes to 400 μL was done with manual or automated pipettors, and re-equilibration was allowed for 30 min. Three rounds of ultrafiltration-based affinity selection were performed, and the ligands were characterized and analyzed by organic solvent extraction and ESI-TOF mass spectrometry as described.²⁹ The mixtures were screened in duplicate. Screening and compound extraction were performed in 1 day, and mass spectrometry also was carried out in a single day using automated sample handling. Analyses of the mass spectra and selection of putative ligands for deconvolution were performed using custom software.²⁹ In the second stage, putative ligands were selected from the primary screen, freshly prepared into new mixtures with no mass redundancy and rescreened for confirmation of binding. In order to exclude false positive artifacts due to aggregation^{54–56} or other non-protein-dependent mechanisms, selection experiments also were conducted on the small mixtures in the absence of protein.^{28,29} The entire process to screen one protein through both stages required approximately 3 weeks, including time for analysis and obtaining compounds from a liquid sample management system.

NMR Binding Studies. NMR samples consisted of ^{13}C -methyl-labeled⁵³ Jnk-1 (residues 1–364, T183E, Y185E) in a buffer containing 20 mM Tris, 150 mM NaCl, 2 mM DTT, and 5 mM MgCl₂, pH 8.0, and ^{13}C -methyl-labeled⁵³ p38 α (residues 1–360) in buffer comprising 50 mM Tris, pH 7.5, and 2 mM DTT. Ligand binding was detected by acquiring $^1\text{H}/^{13}\text{C}$ -HSQC spectra utilizing a WATERGATE sequence⁵⁷ for solvent suppression on 500 μL of 0.04 mM protein in the presence and absence of added compound. A Bruker sample changer was used on a Bruker DRX500 spectrometer equipped with a Cryo-Probe.⁵⁸ Binding was determined by the observation of changes in the HSQC spectrum. NMR methyl assignments for Jnk-1 were obtained through site-directed mutagenesis.

X-ray Crystallographic Studies on Jnk-1. Good quality crystals of JNK1- α 1⁵⁹ with a C-His-tag extension were obtained under the conditions described previously.²³ The crystals of the apo-JNK1- α 1 were characterized as trigonal ($P3_121$ or enantiomer) with cell constants of $a = b = 155.9\text{ \AA}$, $c = 124.5\text{ \AA}$ and diffracted to 3.5 \AA resolution in house and to about 3.0 \AA at the advanced photon source (APS; beamline ID-17, IMCA-CAT). Isomorphous co-crystals of

Jnk-1 with one of the non-ATP inhibitors (a biaryl tetrazole (compound 2) IC₅₀ $\sim 8\text{ }\mu\text{M}$) were also characterized ($a = b = 158.4\text{ \AA}$, $c = 123.9\text{ \AA}$) at the APS, diffracting to 2.7 \AA resolution. The slight difference in the cell parameters reflects the minor structural changes induced in the protein by the presence of the inhibitor at the non-ATP site. Both crystals were grown in the presence of the undecapeptide (R-P-K-R-P-T-T-L-N-L-F) derived from the JIP1 scaffolding protein (JIP1(153–163))⁶⁰ with protocols similar to the ones described.¹⁷ Crystallographic statistics for apo Jnk-1 and the compound 3/Jnk-1 complex are included in Supplementary Table 1.

The structure of Jnk-1 in the apo form was solved by molecular replacement using the structure of the related kinase Jnk-3³⁰ (PDB entry 1jnk; residues 63–373) and the software package MOLREP⁶¹ as implemented in the CCP4 program suite.⁶² Although the cell volume was large enough to accommodate four Jnk-1 molecules in the asymmetric unit, the best molecular replacement solution ($R = 0.55$, correlation coefficient = 0.52 for data between 20–3.8 \AA resolution) suggested only two molecules/au packed in space group $P3_121$. Subsequent refinement by cycles of manual revision and crystallographic refinement using CNX confirmed this tentative solution, and the resulting electron density maps showed density corresponding to the JIP1 peptide as reported earlier.¹⁷ The refinement was continued by conventional methods ($R_{\text{work}} = 0.247$, $R_{\text{free}} = 0.298$ to a resolution of 3.0 \AA). Co-crystals of Jnk-1 and biaryl tetrazole compounds typically diffracted to better resolution (2.7 \AA) than the apo- Jnk-1. The structure of the complex was solved by molecular replacement using the refined structure of the apo Jnk-1 protein as a model and refined by conventional protocols to a final $R_{\text{work}} = 0.242$ ($R_{\text{free}} = 0.281$). Coordinates for the refined structures of apo Jnk-1 and the complex with compound 3 have been deposited with the Protein Data Bank,⁶³ with entry codes 3O17 and 3O2M, respectively.

Biacore Studies. Experiments were performed with a Biacore T100 instrument using a CMS sensor chip (Biacore AB). Unphosphorylated p38 α protein was first exchanged into sodium phosphate buffer, pH 7.5 with 5 mM DTT and then immobilized by direct amine coupling. Since the protein is not stable at low pH, 10 μM of compound 9 was added to the protein before diluting into 10 mM sodium acetate (pH 5.5) buffer. Typical immobilization levels were 6000–7000 RU. Compound 9 was used as positive control to evaluate the active surface on the chip. About 20% the surface was calculated to be active (capable of binding compounds) on the basis of the R_{max} obtained for compound 9 (15–20 RU). A buffer containing 10 mM HEPES, pH 7.4, 150 mM NaCl, 3 mM DTT, 0.05% Tween-20, 10 mM MgCl₂, and 1 mM DTT was used as running buffer.

X-ray Crystallographic Studies on p38 α . Human p38 α protein containing a C162S mutation was used for co-crystallization with compound 10. Protein was expressed in *E. coli* with an N-terminal 6-His-thrombin cleavage site tag, purified by affinity Ni²⁺-NTA column followed by an thrombin cleavage, ion-exchange chromatography on a Source Q column (GE), and size exclusion chromatography.

Crystals of p38 α were obtained by the hanging drop method at a protein concentration of 30 mg mL⁻¹ in 25 mM Tris pH 8, 100 mM NaCl, 10% glycerol, and 10 mM DTT co-crystallized with 1 mM compound 10 in 20% PEG 2000MME and 0.1 M Bis-Tris pH 6.5 at 18 $^\circ\text{C}$. A crystal was frozen in 20% PEG 2000MME, 0.1 M Bis-Tris pH 7.5, and 15% ethylene glycol, and X-ray data were collected at the APS. The crystal belonged to an orthorhombic space group ($P2_12_12_1$) with $a = 64.9\text{ \AA}$, $b = 74.5\text{ \AA}$, and $c = 77.9\text{ \AA}$ and diffracted to 2.5 \AA . The structure was solved by molecular replacement (CCP4i)⁶⁴ using the apo-form of p38 α .⁴⁵ Electron density for the compound around the MAP kinase insert region was clearly visible in maps viewed in O ,⁶⁵ and the conformation of residues Met194 to Met198 in the apo-structure was rebuilt. Compound 10 was docked into the electron density in this pocket using AFIT (OpenEye Scientific Software). Weak density was also observed in the ATP-binding site, but it was not possible to

determine if this density was due to binding of compound 10. Refinement of the model was done in REFMAC⁶⁶ resulting in $R_{\text{free}} = 0.305$ and $R_{\text{cryst}} = 0.214$. Coordinates for p38 α complexed with compound 10 have been deposited with the Protein Data Bank⁶³ with entry code 3NEW. Crystallographic statistics for the compound 10/p38 α complex are included in Supplementary Table 2.

Chemical Synthesis. The synthesis of 1 has been previously published.²⁴ Compounds 2 and 3 also have been previously described.⁶⁷ Compound 7 can be synthesized in a straightforward fashion as shown in Supplementary Scheme 1. Briefly, acid-catalyzed condensation of aminothiazole with *p*-anisaldehyde yielded the Schiff base intermediate, which was reduced with sodium borohydride to provide the secondary amine. Alkylation with *p*-fluorobenzyl bromide and demethylation with boron tribromide generated the desired compound. The related analogues can be prepared in a similar manner (see Supporting Information).

■ ASSOCIATED CONTENT

S Supporting Information. This material is available free of charge via the Internet at <http://pubs.acs.org>.

■ AUTHOR INFORMATION

Corresponding Author

*kenneth.m.comess@abbott.com

■ ACKNOWLEDGMENT

The authors wish to express their appreciation to the members of the Metabolic Diseases and Protein Crystallography research groups at Abbott and P. Richardson and L. Barrett for preparing the JIP peptide used in the crystallographic studies. Additional experimental support was provided by J. Trevillyan, E. Olejniczak, E. Matayoshi, S. Dorwin, J. Harlan, U. Lador, L. Solomon, K. Haskins, D. Bartley, and K. Walter.

■ REFERENCES

- (1) Zhang, J., Yang, P. L., and Gray, N. S. (2009) Targeting cancer with small molecule kinase inhibitors. *Nat. Rev. Cancer* 9, 28–39.
- (2) Landry, Y., and Gies, J. P. (2008) Drugs and their molecular targets: an updated overview. *Fundam. Clin. Pharmacol.* 22, 1–18.
- (3) Fabian, M. A., Biggs, W. H., 3rd, Treiber, D. K., Atteridge, C. E., Azimioara, M. D., Benedetti, M. G., Carter, T. A., Ciceri, P., Edeen, P. T., Floyd, M., Ford, J. M., Galvin, M., Gerlach, J. L., Grotzfeld, R. M., Herrgard, S., Insko, D. E., Insko, M. A., Lai, A. G., Lelias, J. M., Mehta, S. A., Milanov, Z. V., Velasco, A. M., Wodicka, L. M., Patel, H. K., Zarrinkar, P. P., and Lockhart, D. J. (2005) A small molecule-kinase interaction map for clinical kinase inhibitors. *Nat. Biotechnol.* 23, 329–336.
- (4) Oishi, J., Han, X., Kang, J.-H., Asami, Y., Mori, T., Niidome, T., and Katayama, Y. (2008) High-throughput colorimetric detection of tyrosine kinase inhibitors based on the aggregation of gold nanoparticles. *Anal. Biochem.* 373, 161–163.
- (5) Card, A., Caldwell, C., Min, H., Lokchander, B., Hualin, X., Sciabola, S., Kamath, A. V., Clugston, S. L., Tschantz, W. R., Leyu, W., and Moshinsky, D. J. (2009) High-throughput biochemical kinase selectivity assays: panel development and screening applications. *J. Biomol. Screening* 14, 31–42.
- (6) Hopkins, A. L., Mason, J. S., and Overington, J. P. (2006) Can we rationally design promiscuous drugs? *Curr. Opin. Struct. Biol.* 16, 127–136.
- (7) Bilanges, B., Torbett, N., and Vanhaesebroeck, B. (2008) Killing two kinase families with one stone. *Nat. Chem. Biol.* 4, 648–649.
- (8) Manning, G., Whyte, D. B., Martinez, R., Hunter, T., and Sudarsanam, S. (2002) The protein kinase complement of the human genome. *Science* 298, 1912–1934.
- (9) Fedorov, O., Marsden, B., Pogacic, V., Rellos, P., Muller, S., Bullock, A. N., Schwaller, J., Sundstrom, M., and Knapp, S. (2007) A systematic interaction map of validated kinase inhibitors with Ser/Thr kinases. *Proc. Natl. Acad. Sci. U.S.A.* 104, 20523–20528.
- (10) Widakowich, C., de Castro, G., Jr., de Azambuja, E., Dinh, P., and Awada, A. (2007) Review: side effects of approved molecular targeted therapies in solid cancers. *Oncologist* 12, 1443–1455.
- (11) Akritopoulou-Zanze, I., and Hajduk, P. J. (2009) Kinase-targeted libraries: the design and synthesis of novel, potent, and selective kinase inhibitors. *Drug Discovery Today* 14, 291–297.
- (12) Bogoyevitch, M. A., and Arthur, P. G. (2008) Inhibitors of c-Jun N-terminal kinases: JuNK no more? *Biochim. Biophys. Acta* 1784, 76–93.
- (13) Aguirre, V., Uchida, T., Yenush, L., Davis, R., and White, M. F. (2000) The c-Jun NH(2)-terminal kinase promotes insulin resistance during association with insulin receptor substrate-1 and phosphorylation of Ser(307). *J. Biol. Chem.* 275, 9047–9054.
- (14) Aguirre, V., Werner, E. D., Giraud, J., Lee, Y. H., Shoelson, S. E., and White, M. F. (2002) Phosphorylation of Ser307 in insulin receptor substrate-1 blocks interactions with the insulin receptor and inhibits insulin action. *J. Biol. Chem.* 277, 1531–1537.
- (15) Hirosumi, J., Tuncman, G., Chang, L., Gorgun, C. Z., Uysal, K. T., Maeda, K., Karin, M., and Hotamisligil, G. S. (2002) A central role for JNK in obesity and insulin resistance. *Nature* 420, 333–336.
- (16) Bennett, B. L., Sasaki, D. T., Murray, B. W., O'Leary, E. C., Sakata, S. T., Xu, W., Leisten, J. C., Motiwala, A., Pierce, S., Satoh, Y., Bhagwat, S. S., Manning, A. M., and Anderson, D. W. (2001) SP600125, an anthracycline inhibitor of Jun N-terminal kinase. *Proc. Natl. Acad. Sci. U.S.A.* 98, 13681–13686.
- (17) Heo, Y. S., Kim, S. K., Seo, C. I., Kim, Y. K., Sung, B. J., Lee, H. S., Lee, J. I., Park, S. Y., Kim, J. H., Hwang, K. Y., Hyun, Y. L., Jeon, Y. H., Ro, S., Cho, J. M., Lee, T. G., and Yang, C. H. (2004) Structural basis for the selective inhibition of JNK1 by the scaffolding protein JIP1 and SP600125. *EMBO J.* 23, 2185–2195.
- (18) Kaneto, H., Nakatani, Y., Miyatsuka, T., Kawamori, D., Matsuoka, T. A., Matsuhisa, M., Kajimoto, Y., Ichijo, H., Yamasaki, Y., and Hori, M. (2004) Possible novel therapy for diabetes with cell-permeable JNK-inhibitory peptide. *Nat. Med.* 10, 1128–1132.
- (19) Ruckle, T., Biamonte, M., Grippi-Vallotton, T., Arkininstall, S., Cambet, Y., Camps, M., Chabert, C., Church, D. J., Halazy, S., Jiang, X., Martinou, I., Nichols, A., Sauer, W., and Gotteland, J. P. (2004) Design, synthesis, and biological activity of the first generation of novel potent, selective (benzoylaminoethyl)thiophene sulfonamide inhibitors of c-Jun-N-terminal kinase. *J. Med. Chem.* 47, 6921–6934.
- (20) Gaillard, P., Jeanclaude-Etter, I., Ardisson, V., Arkininstall, S., Cambet, Y., Camps, M., Chabert, C., Church, D., Cirillo, R., Gretener, D., Halazy, S., Nichols, A., Szyndralewicz, C., Vitte, P. A., and Gotteland, J. P. (2005) Design and synthesis of the first generation of novel potent, selective, and in vivo active (benzothiazol-2-yl)acetone nitrile inhibitors of the c-Jun N-terminal kinase. *J. Med. Chem.* 48, 4596–4607.
- (21) Stocks, M. J., Barber, S., Ford, R., Leroux, F., St-Gallay, S., Teague, S., and Xue, Y. (2005) Structure-driven HtL: design and synthesis of novel aminoindazole inhibitors of c-Jun N-terminal kinase activity. *Bioorg. Med. Chem. Lett.* 15, 3459–3462.
- (22) Liu, M., Xin, Z., Clampit, J. E., Wang, S., Gum, R. J., Haasch, D. L., Trevillyan, J. M., Abad-Zapatero, C., Fry, E. H., Sham, H. L., and Liu, G. (2006) Synthesis and SAR of 1,9-dihydro-9-hydroxypyrazolo-[3,4-*b*]quinolin-4-ones as novel, selective c-Jun N-terminal kinase inhibitors. *Bioorg. Med. Chem. Lett.* 16, 2590–2594.
- (23) Szczepankiewicz, B. G., Kosogof, C., Nelson, L. T., Liu, G., Liu, B., Zhao, H., Serby, M. D., Xin, Z., Liu, M., Gum, R. J., Haasch, D. L., Wang, S., Clampit, J. E., Johnson, E. F., Lubben, T. H., Stashko, M. A., Olejniczak, E. T., Sun, C., Dorwin, S. A., Haskins, K., Abad-Zapatero, C., Fry, E. H., Hutchins, C. W., Sham, H. L., Rondinone, C. M., and Trevillyan, J. M. (2006) Aminopyridine-based c-Jun N-terminal kinase inhibitors with cellular activity and minimal cross-kinase activity. *J. Med. Chem.* 49, 3563–3580.
- (24) Zhao, H., Serby, M. D., Xin, Z., Szczepankiewicz, B. G., Liu, M., Kosogof, C., Liu, B., Nelson, L. T., Johnson, E. F., Wang, S., Pederson, T.,

- Gum, R. J., Clampit, J. E., Haasch, D. L., Abad-Zapatero, C., Fry, E. H., Rondinone, C., Trevillyan, J. M., Sham, H. L., and Liu, G. (2006) Discovery of potent, highly selective, and orally bioavailable pyridine carboxamide c-Jun NH₂-terminal kinase inhibitors. *J. Med. Chem.* 49, 4455–4458.
- (25) Liu, M., Wang, S., Clampit, J. E., Gum, R. J., Haasch, D. L., Rondinone, C. M., Trevillyan, J. M., Abad-Zapatero, C., Fry, E. H., Sham, H. L., and Liu, G. (2007) Discovery of a new class of 4-anilinopyrimidines as potent c-Jun N-terminal kinase inhibitors: Synthesis and SAR studies. *Bioorg. Med. Chem. Lett.* 17, 668–672.
- (26) Asano, Y., Kitamura, S., Ohra, T., Aso, K., Igata, H., Tamura, T., Kawamoto, T., Tanaka, T., Sogabe, S., Matsumoto, S., Yamaguchi, M., Kimura, H., and Itoh, F. (2008) Discovery, synthesis and biological evaluation of isoquinolones as novel and highly selective JNK inhibitors (1). *Bioorg. Med. Chem.* 16, 4715–4732.
- (27) Stebbins, J. L., De, S. K., Machleidt, T., Becattini, B., Vazquez, J., Kuntzen, C., Chen, L. H., Cellitti, J. F., Riel-Mehan, M., Emdadi, A., Solinas, G., Karin, M., and Pellecchia, M. (2008) Identification of a new JNK inhibitor targeting the JNK-JIP interaction site. *Proc. Natl. Acad. Sci. U.S.A.* 105, 16809–16813.
- (28) Comess, K. M., Schurdak, M. E., Voorbach, M. J., Coen, M., Trumbull, J. D., Yang, H., Gao, L., Tang, H., Cheng, X., Lerner, C. G., McCall, J. O., Burns, D. J., and Beutel, B. A. (2006) An ultraefficient affinity-based high-throughput screening process: application to bacterial cell wall biosynthesis enzyme MurF. *J. Biomol. Screening* 11, 743–754.
- (29) Comess, K. M., Trumbull, J. D., Park, C., Chen, Z., Judge, R. A., Voorbach, M. J., Coen, M., Gao, L., Tang, H., Kovar, P., Cheng, X., Schurdak, M. E., Zhang, H., Sowin, T., and Burns, D. J. (2006) Kinase drug discovery by affinity selection/mass spectrometry (ASMS): application to DNA damage checkpoint kinase Chk1. *J. Biomol. Screening* 11, 755–764.
- (30) Xie, X., Gu, Y., Fox, T., Coll, J. T., Fleming, M. A., Markland, W., Caron, P. R., Wilson, K. P., and Su, M. S. (1998) Crystal structure of JNK3: a kinase implicated in neuronal apoptosis. *Structure* 6, 983–991.
- (31) Scapin, G., Patel, S. B., Lisnock, J., Becker, J. W., and LoGrasso, P. V. (2003) The structure of JNK3 in complex with small molecule inhibitors: structural basis for potency and selectivity. *Chem. Biol.* 10, 705–712.
- (32) Dominguez, C., Powers, D. A., and Tamayo, N. (2005) p38 MAP kinase inhibitors: many are made, but few are chosen. *Curr. Opin. Drug Discovery Dev.* 8, 421–430.
- (33) Genovese, M. C. (2009) Inhibition of p38: Has the fat lady sung? *Arthritis Rheum.* 60, 317–320.
- (34) Cottrell, J. A., Meyenhofer, M., Medicherla, S., Higgins, L., and O'Connor, J. P. (2009) Analgesic effects of p38 kinase inhibitor treatment on bone fracture healing. *Pain* 142, 116–126.
- (35) Davies, S. P., Reddy, H., Caivano, M., and Cohen, P. (2000) Specificity and mechanism of action of some commonly used protein kinase inhibitors. *Biochem. J.* 351, 95–105.
- (36) Lee, M. R., and Dominguez, C. (2005) MAP kinase p38 inhibitors: clinical results and an intimate look at their interactions with p38alpha protein. *Curr. Med. Chem.* 12, 2979–2994.
- (37) Pargellis, C., Tong, L., Churchill, L., Cirillo, P. F., Gilmore, T., Graham, A. G., Grob, P. M., Hickey, E. R., Moss, N., Pav, S., and Regan, J. (2002) Inhibition of p38 MAP kinase by utilizing a novel allosteric binding site. *Nat. Struct. Biol.* 9, 268–272.
- (38) Coleman, R. G., Salzberg, A. C., and Cheng, A. C. (2006) Structure-based identification of small molecule binding sites using a free energy model. *J. Chem. Inf. Model* 46, 2631–2637.
- (39) Jackson, J. R., Bolognese, B., Hillegass, L., Kassis, S., Adams, J., Griswold, D. E., and Winkler, J. D. (1998) Pharmacological effects of SB 220025, a selective inhibitor of P38 mitogen-activated protein kinase, in angiogenesis and chronic inflammatory disease models. *J. Pharmacol. Exp. Ther.* 284, 687–692.
- (40) Karaman, M. W., Herrgard, S., Treiber, D. K., Gallant, P., Atteridge, C. E., Campbell, B. T., Chan, K. W., Ciceri, P., Davis, M. I., Edeen, P. T., Faraoni, R., Floyd, M., Hunt, J. P., Lockhart, D. J., Milanov, Z. V., Morrison, M. J., Pallares, G., Patel, H. K., Pritchard, S., Wodicka, L. M., and Zarrinkar, P. P. (2008) A quantitative analysis of kinase inhibitor selectivity. *Nat. Biotechnol.* 26, 127–132.
- (41) Cuenda, A., Rouse, J., Doza, Y. N., Meier, R., Cohen, P., Gallagher, T. F., Young, P. R., and Lee, J. C. (1995) SB 203580 is a specific inhibitor of a MAP kinase homologue which is stimulated by cellular stresses and interleukin-1. *FEBS Lett.* 364, 229–233.
- (42) Wang, Z., Harkins, P. C., Ulevitch, R. J., Han, J., Cobb, M. H., and Goldsmith, E. J. (1997) The structure of mitogen-activated protein kinase p38 at 2.1-Å resolution. *Proc. Natl. Acad. Sci. U.S.A.* 94, 2327–2332.
- (43) Diskin, R., Engelberg, D., and Livnah, O. (2008) A novel lipid binding site formed by the MAP kinase insert in p38 alpha. *J. Mol. Biol.* 375, 70–79.
- (44) Wang, Z., Canagarajah, B. J., Boehm, J. C., Kassisa, S., Cobb, M. H., Young, P. R., Abdel-Meguid, S., Adams, J. L., and Goldsmith, E. J. (1998) Structural basis of inhibitor selectivity in MAP kinases. *Structure* 6, 1117–1128.
- (45) Wilson, K. P., Fitzgibbon, M. J., Caron, P. R., Griffith, J. P., Chen, W., McCaffrey, P. G., Chambers, S. P., and Su, M. S. (1996) Crystal structure of p38 mitogen-activated protein kinase. *J. Biol. Chem.* 271, 27696–27700.
- (46) White, A., Pargellis, C. A., Studts, J. M., Werneburg, B. G., and Farmer, B. T., 2nd (2007) Molecular basis of MAPK-activated protein kinase 2:p38 assembly. *Proc. Natl. Acad. Sci. U.S.A.* 104, 6353–6358.
- (47) Lebakken, C. S., Riddle, S. M., Singh, U., Frazee, W. J., Eliason, H. C., Gao, Y., Reichling, L. J., Marks, B. D., and Vogel, K. W. (2009) Development and applications of a broad-coverage, TR-FRET-based kinase binding assay platform. *J. Biomol. Screening* 14, 924–935.
- (48) Huth, J. R., Yu, L., Collins, I., Mack, J., Mendoza, R., Isaac, B., Braddock, D. T., Muchmore, S. W., Comess, K. M., Fesik, S. W., Clore, G. M., Levens, D., and Hajduk, P. J. (2004) NMR-driven discovery of benzoylanthranilic acid inhibitors of far upstream element binding protein binding to the human oncogene c-myc promoter. *J. Med. Chem.* 47, 4851–4857.
- (49) Qjan, J., Voorbach, M. J., Huth, J. R., Coen, M. L., Zhang, H., Ng, S.-C., Comess, K. M., Petros, A. M., Rosenberg, S. H., Warrior, U., and Burns, D. J. (2004) Discovery of novel inhibitors of Bcl-xL using multiple high-throughput screening platforms. *Anal. Biochem.* 328, 131–138.
- (50) Kawai, M., BaMaung, N. Y., Fidanze, S. D., Erickson, S. A., Tedrow, J. S., Sanders, W. J., Vasudevan, A., Park, C., Hutchins, C., Comess, K. M., Kalvin, D., Wang, J., Zhang, Q., Lou, P., Tucker-Garcia, L., Bouska, J., Bell, R. L., Lesniewski, R., Henkin, J., and Sheppard, G. S. (2006) Development of sulfonamide compounds as potent methionine aminopeptidase type II inhibitors with antiproliferative properties. *Bioorg. Med. Chem. Lett.* 16, 3574–3577.
- (51) Lerner, C. G., Hajduk, P. J., Wagner, R., Wagenaar, F. L., Woodall, C., Gu, Y. G., Searle, X. B., Florjancic, A. S., Zhang, T., Clark, R. F., Cooper, C. S., Mack, J. C., Yu, L., Cai, M., Betz, S. F., Chovan, L. E., McCall, J. O., Black-Schaefer, C. L., Kakavas, S. J., Schurdak, M. E., Comess, K. M., Walter, K. A., Edalji, R., Dorwin, S. A., Smith, R. A., Hebert, E. J., Harlan, J. E., Metzger, R. E., Merta, P. J., Baranowski, J. L., Coen, M. L., Thornewell, S. J., Shivakumar, A. G., Saiki, A. Y., Soni, N., Bui, M., Balli, D. J., Sanders, W. J., Nilius, A. M., Holzman, T. F., Fesik, S. W., and Beutel, B. A. (2007) From bacterial genomes to novel antibacterial agents: discovery, characterization, and antibacterial activity of compounds that bind to HI0065 (YjeE) from *Haemophilus influenzae*. *Chem. Biol. Drug Des.* 69, 395–404.
- (52) Wendt, M. D., Sun, C., Kunzer, A., Sauer, D., Sarris, K., Hoff, E., Yu, L., Nettesheim, D. G., Chen, J., Jin, S., Comess, K. M., Fan, Y., Anderson, S. N., Isaac, B., Olejniczak, E. T., Hajduk, P. J., Rosenberg, S. H., and Elmore, S. W. (2007) Discovery of a novel small molecule binding site of human survivin. *Bioorg. Med. Chem. Lett.* 17, 3122–3129.
- (53) Hajduk, P. J., Augeri, D. J., Mack, J., Mendoza, R., Yang, J., Betz, S. F., and Fesik, S. W. (2000) NMR-Based screening of proteins containing ¹³C-labeled methyl groups. *J. Am. Chem. Soc.* 122, 7898–7904.

- (54) Seidler, J., McGovern, S. L., Doman, T. N., and Shoichet, B. K. (2003) Identification and prediction of promiscuous aggregating inhibitors among known drugs. *J. Med. Chem.* *46*, 4477–4486.
- (55) Feng, B. Y., and Shoichet, B. K. (2006) Synergy and antagonism of promiscuous inhibition in multiple-compound mixtures. *J. Med. Chem.* *49*, 2151–2154.
- (56) Shoichet, B. K. (2006) Screening in a spirit haunted world. *Drug Discovery Today* *11*, 607–615.
- (57) Piotto, M., Saudek, V., and Sklenar, V. (1992) Gradient-tailored excitation for single-quantum NMR spectroscopy of aqueous solutions. *J. Biomol. NMR* *2*, 661–665.
- (58) Hajduk, P. J., Gerfin, T., Boehlen, J. M., Haberli, M., Marek, D., and Fesik, S. W. (1999) High-throughput nuclear magnetic resonance-based screening. *J. Med. Chem.* *42*, 2315–2317.
- (59) Gupta, S., Barrett, T., Whitmarsh, A. J., Cavanagh, J., Sluss, H. K., Derijard, B., and Davis, R. J. (1996) Selective interaction of JNK protein kinase isoforms with transcription factors. *EMBO J.* *15*, 2760–2770.
- (60) Barr, R. K., Kendrick, T. S., and Bogoyevitch, M. A. (2002) Identification of the critical features of a small peptide inhibitor of JNK activity. *J. Biol. Chem.* *277*, 10987–10997.
- (61) Vagin, A., and Teplyakov, A. (1997) MOLREP: an automated program for molecular replacement. *J. Appl. Crystallogr.* *30*, 1022–1025.
- (62) CCP4. (1994) The CCP4 Suite: Programs for protein crystallography. *Acta Crystallogr., Sect. D: Biol. Crystallogr.* *D50*, 760–763.
- (63) Berman, H. M., Westbrook, J., Feng, Z., Gilliland, G., Bhat, T. N., Weissig, H., Shindyalov, I. N., and Bourne, P. E. (2000) The Protein Data Bank. *Nucleic Acids Res.* *28*, 235–242.
- (64) Potterton, E., Briggs, P., Turkenburg, M., and Dodson, E. (2003) A graphical user interface to the CCP4 program suite. *Acta Crystallogr. Sect. D: Biol. Crystallogr.* *59*, 1131–1137.
- (65) Jones, T. A., Zou, J. Y., Cowan, S. W., and Kjeldgaard (1991) Improved methods for building protein models in electron density maps and the location of errors in these models. *Acta Crystallogr., Sect. A: Found. Crystallogr.* *47*, 110–119.
- (66) Murshudov, G. N., Vagin, A. A., and Dodson, E. J. (1997) Refinement of macromolecular structures by the maximum-likelihood method. *Acta Crystallogr. D57*, 240–255.
- (67) De, B., Winn, M., Zydowsky, T. M., Kerkman, D. J., DeBernardis, J. F., Lee, J., Buckner, S., Warner, R., Brune, M., Hancock, A., Opgenorth, T., and Marsh, K. (1992) Discovery of a novel class of orally active, non-peptide angiotensin II antagonists. *J. Med. Chem.* *35*, 3714–3717.